Ecotoxicology and Environmental Safety 150 (2018) 199–206

Contents lists available at ScienceDirect

Ecotoxicology and Environmental Safety

journal homepage: www.elsevier.com/locate/ecoenv

n-Alkanes in sediments from the Yellow River Estuary, China: Occurrence, sources and historical sedimentary record

Shanshan Wang[a,b], Guijian Liu[a,b,*], Zijiao Yuan[a], Chunnian Da[a]

[a] CAS Key Laboratory of Crust-Mantle Materials and the Environment, School of Earth and Space Sciences, University of Science and Technology of China, Hefei 230026, China

[b] State Key Laboratory of Loess and Quaternary Geology, Institute of Earth Environment, The Chinese Academy of Sciences, Xi'an 710075, Shaanxi, China

ARTICLE INFO

Keywords:
n-Alkanes
Surface sediments
Sediment core
Yellow River Estuary
Old Yellow River Estuary

ABSTRACT

A total of 21 surface sediments from the Yellow River Estuary (YRE) and a sediment core from the abandoned Old Yellow River Estuary (OYRE) were analyzed for *n*-alkanes using gas chromatography-mass spectrometry (GC-MS). *n*-Alkanes in the range C_{12}-C_{33} and C_{13}-C_{34} were identified in the surface sediments and the core, respectively. The homologous series were mainly bimodal distribution pattern without odd/even predominance in the YRE and OYRE. The total *n*-alkanes concentrations in the surface sediments ranged from 0.356 to 0.572 mg/kg, with a mean of 0.434 mg/kg on dry wt. basis. Evaluation of *n*-alkanes proxies indicated that the aliphatic hydrocarbons in the surface sediments were derived mainly from a petrogenic source with a relatively low contribution of submerged/floating macrophytes, terrestrial and emergent plants. The dated core covered the time period 1925–2012 and the mean sedimentation rate was ca. 0.5 cm/yr. The total *n*-alkanes concentrations in the core ranged from 0.0394 to 0.941 mg/kg, with a mean of 0.180 mg/kg. The temporal evolution of *n*-alkanes reflected the historical input of aliphatic hydrocarbons and was consistent with local and regional anthropogenic activity. In general, the investigation on the sediment core revealed a trend of regional environmental change and the role of anthropogenic activity in environmental change.

1. Introduction

Coastal and estuarine regions are areas where active interaction between land and ocean exists (Wang et al., 2015). In recent decades, the impact of industrial discharge, agricultural emission and other anthropogenic activities have been extremely prominent in coastal and estuarine regions. Aliphatic hydrocarbons, which widespread in the estuarine region, have aroused extensive attention worldwide (e.g. Hu et al., 2011; Wang et al., 2015). Estuarine sediments are a major reservoir of aliphatic hydrocarbons from anthropogenic input and natural input (Hostettler et al., 1999; Tahir et al., 2015; Wu et al., 2001). Due to their hydrophobic nature, aliphatic hydrocarbons generally have a high tendency to adhere to particles (Guo et al., 2011; Silva et al., 2013). Eventually, they may accumulate in estuarine areas through riverine runoff and/or atmospheric deposition and be preserved in sediments for a long period of time (Hostettler et al., 1999; Wang et al., 2015). Therefore, the analysis of sediment cores is an efficient way of reconstructing the depositional history of aliphatic hydrocarbons and environmental changes in estuarine environments (Hostettler et al., 1999).

Aliphatic hydrocarbons such as *n*-alkanes are released to the environment primarily through anthropogenic (vehicle exhaust, petroleum and industrial releases) and natural sources (aquatic organisms, plankton and terrestrial plants) (Wang et al., 2012a). *n*-Alkanes in sediments are widely used as a sensitive indicator for source identification of aliphatic hydrocarbons (Ho et al., 2015; Wang et al., 2017; Zhang et al., 2009). Although they only account for a small fraction of the aliphatic hydrocarbons, their composition keeps a sufficient record of information regarding the source and maturity of aliphatic hydrocarbons (Hostettler et al., 1999; Kaiser et al., 2014).

The Yellow River has flowed into the Bohai Sea since 1855 from Shandong Province, North China. The Yellow River Delta (YRD) has plentiful wetland and biological resources, with tremendous developing potentiality and ecological sensitivity (Wang et al., 2011). Moreover, it is also an important oil-producing base for China (Nie et al., 2009). The Shengli Oilfield was discovered in the YRD in the 1960s, accelerating industrialization and promoting the economic development of China. However, with the development of the oil industry, the estuarine wetland ecosystem has been significantly affected by oil exploration, transportation, storage and consumption. Aliphatic hydrocarbons and

* Corresponding author at: CAS Key Laboratory of Crust-Mantle Materials and the Environment, School of Earth and Space Sciences, University of Science and Technology of China, Hefei 230026, China.
E-mail address: lgj@ustc.edu.cn (G. Liu).

https://doi.org/10.1016/j.ecoenv.2017.12.016
Received 10 August 2017; Received in revised form 1 December 2017; Accepted 9 December 2017
Available online 04 January 2018

other oil-related organic pollutants have been released into the wetland ecosystem and may cause a health risk to humans and living organisms.

The course of the Yellow River was frequently diverted after 1855, owing to the effect of natural and human factors. An artificial diversion was conducted to relocate the course from Diaokou to Qingshuigou channel in 1976 (Wang et al., 2006a). Since then, the Old Yellow River Estuary (OYRE) has served the river for 20 yr (1976–1996). The terminal channel of the Yellow River shifted to the current course in 1996. The Yellow River has flowed through the Yellow River Estuary (YRE) into the sea until now. Various anthropogenic activities in the OYRE and YRE, including industrial discharge, domestic sewage, agricultural activity and shipping activity, may cause a negative impact on the ecological environment. In addition, the OYRE has experienced two major shifts of river channel in the past decades, which may have the potential to change the concentration and source of aliphatic hydrocarbons in estuarine sediments. Therefore, it is necessary to investigate the effect of socio-economic development as well as local and regional anthropogenic activity on ecological environment in the OYRE and call attention to the protection of wetland ecological environment.

However, previous researches have been focused on the YRD and the present YRE (Nie et al., 2010; Wang et al., 2011; Yamei et al., 2009; Yu et al., 2011; Zhang et al., 2009). There are few studies of the aliphatic hydrocarbons in both the present YRE and the OYRE. The major objectives of the present study were to solve the following problems: What are the sources of aliphatic hydrocarbons in the sediments? Has the exploitation of the Shengli Oilfield and the relocation of the course of the Yellow River changed the input sources of the aliphatic hydrocarbons?

The study was designed to (i) estimate potential sources and concentration of *n*-alkanes in the surface sediments from the present YRE and the sediment core from the OYRE and (ii) investigate any correlation between anthropogenic activity and environmental change over the last eight decades. It was hoped that the results may provide valuable insight into understanding the role of human activity in environmental change and a reliable prerequisite for future studies of organic pollutants in the region.

2. Material and methods

2.1. Sample collection

The sampling locations are illustrated in Fig. 1. Surface sediments (21; i.e. S1 to S21) were collected with a stainless steel grab sampler in the YRE in August 2013. In addition, a sediment core was collected from the OYRE (37°39′5.48″N, 119°16′19.15″E) in July 2012, by using a gravity corer with an inner diameter of 80-mm to prevent physical disturbance of the surface sediment layers. Three cores were collected randomly from the same intertidal mud-flat area in the OYRE during sampling and the core without any physical disturbance was selected for use. The selected core, collected from the surface to 41 cm depth, was located at the mouth of the Qingshuigou course, the abandoned course of the Yellow River. It was immediately sectioned into 1 cm intervals using a stainless steel cutter. All the samples, including the surface sediments and the sectioned samples, were transferred to pre-cleaned Al foil. Then these were transported to the laboratory in an ice box and kept frozen at −20 ℃ prior to analysis.

2.2. ^{210}Pb dating of core

Short-lived ^{210}Pb ($t_{1/2}$ = 22.3 years) is applicable for establishing the chronology of short sediment core on a time-scale of ~100 years (Baskaran et al., 2017; Renfro et al., 2016). Therefore, the dating of the studied core was conducted using the ^{210}Pb method as described by Guo et al. (2007) and Wu et al. (2015). The activity of ^{210}Pb, ^{226}Ra, and ^{137}Cs were determined using an Ortec HPGe GWL series well-type detector. Three reference materials (RGU-1, RGTh-1 and RGK-1) from the International Atomic Energy Agency (IAEA) were used for system calibration. The sediment intervals were sealed in centrifuge tubes for over three weeks to allow radioactive equilibration to be reached before radionuclide determination. The ^{210}Pb activity and ^{226}Ra activity were measured via gamma emissions at 46.5 keV and 352 keV, respectively. The ^{137}Cs was measured simultaneously at 662 keV. The activity of the excess ^{210}Pb ($^{210}Pb_{ex}$, Fig. 2) was calculated by subtraction of the ^{226}Ra activity from the total ^{210}Pb activity. The dating and sedimentation rate were calculated using the constant rate of supply (CRS) model (Al-Mur et al., 2017; Enrico et al., 2017).

2.3. Sample extraction and separation

Each freeze-dried sediment sample was ground and homogenized using an agate mortar and pestle. The samples were sieved through a stainless steel sieve (125 mesh). Powdered sediment intervals (5 g dry wt.) and powdered surface sediments (10 g dry wt.) were used for *n*-alkanes extraction. Microwave-assisted solvent extraction (MASE) was used for the surface sediment samples and soxhlet extraction for the core samples. Activated Cu was added to the extracts for

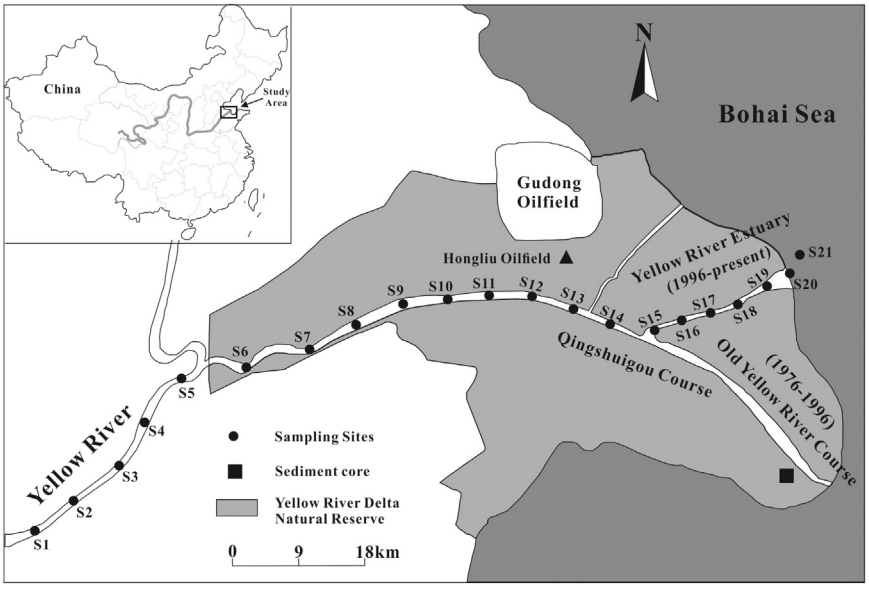

Fig. 1. Sampling locations of the surface sediments and the sediment core in the YRE and OYRE.

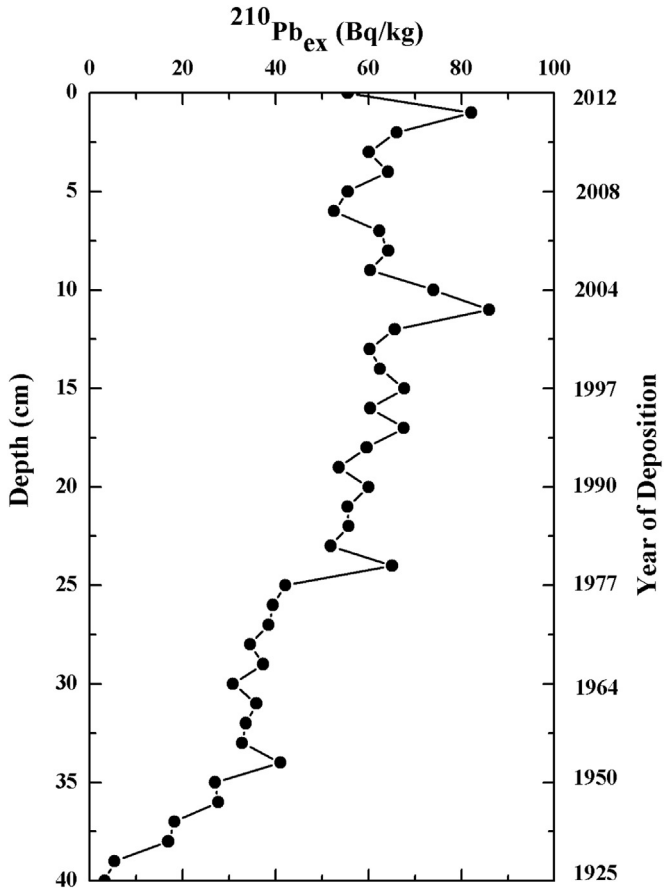

Fig. 2. Depth profile of $^{210}Pb_{ex}$ in the sediment core from the OYRE.

desulfurization. Each extract was concentrated with a vacuum rotary evaporator and then redissolved in hexane. It was purified using a chromatography column filled with alumina (6 cm), silica gel (12 cm) and anhydrous Na_2SO_4 (2 cm) from bottom to top. The *n*-alkanes fraction was eluted with 15 ml hexane and concentrated to 1 ml under a gentle stream of N_2.

2.4. Gas chromatography–mass spectrometry (GC-MS)

Identification and quantification of the *n*-alkanes were carried out using a Thermo Trace Ultra GC unit interfaced to a Thermo DSQ II MS unit, equipped with a TR-5MS column (30 m × 0.25 mm × 0.25 μm). The mass spectrometer was operated in the selective ion monitoring (SIM) mode with positive ion electron impact ionization (EI) mode (70 eV). Samples were injected in splitless mode (1 μl) and high purity helium (99.999%) was used as carrier gas at 1.0 ml/min. The oven temperature program was: 70 ℃ (4 min) to 290 ℃ (held 40 min) at 10 ℃/min. Gas chromatogram of *n*-alkanes was given in Fig. 3.

2.5. Quality assurance and quality control (QA&QC)

The quantification of *n*-alkanes was performed using the external calibration method. To avoid contamination and other interference, QA&QC were conducted strictly for each experimental procedure, including extraction, separation and instrumental analysis. In order to validate the method, recovery experiments were conducted prior to sample extraction. Recovery was determined by adding *n*-alkanes standards to a cleaned matrix (without the target analytes), in the range 75–102%. In addition, a matrix blank (standards added to a cleaned matrix), reagent blank (only solvent), spiked blank (standard added to solvent) and replicate sediment sample were run with each batch of the sediment samples. Analysis of the blanks confirmed that there was no introduced contamination or other interference over the whole experiment. The relative standard deviation was < 5%, indicating good repeatability.

2.6. Statistical analysis

Comparisons of *n*-alkanes concentrations were conducted by independent samples *t*-test using SPSS 17.0 for windows. Statistical differences were considered significant at $p < 0.05$.

Several *n*-alkanes proxies were combined to investigate potential sources of aliphatic hydrocarbons in sediments in the study area. They were calculated from *n*-alkanes abundance based on earlier research as discussed below.

Both the carbon preference index (CPI) and natural *n*-alkane ratio (NAR) are useful for the identification of anthropogenic and biological sources (El Nemr et al., 2013; Mille et al., 2007; Salem et al., 2014). NAR was defined by Mille et al. (2007) as:

$$NAR = \frac{\sum (C_{19} - C_{32}) - 2\sum (C_{20} - C_{32})_{even}}{\sum (C_{19} - C_{32})}$$

CPI was calculated for the entire range of *n*-alkanes, modified according to Górka et al. (2014):

$$CPI\,(C_{12} - C_{33}) = \Sigma (C_{13} - C_{33})_{odd} / \Sigma (C_{12} - C_{32})_{even}$$

The aquatic macrophytes *n*-alkane proxy (P_{aq}) was defined by Ficken et al. (2000) as: $P_{aq} = (C_{23}+C_{25})/(C_{23}+C_{25}+C_{29}+C_{31})$. Emergent and terrestrial plants are characterized by an abundance of long chain *n*-alkanes (C_{29} and/or C_{31}; Ficken et al., 2000). However, non-emergent plants (submerged and floating macrophytes) generally display a dominance of mid chain *n*-alkanes (C_{23} and/or C_{25}; Ficken et al., 2000; Seki et al., 2010). Therefore, P_{aq} can be used to estimate the relative contribution of non-emergent plants vs. emergent and terrestrial plants.

The wax *n*-alkane content (Wax C_n) was calculated (Górka et al.,

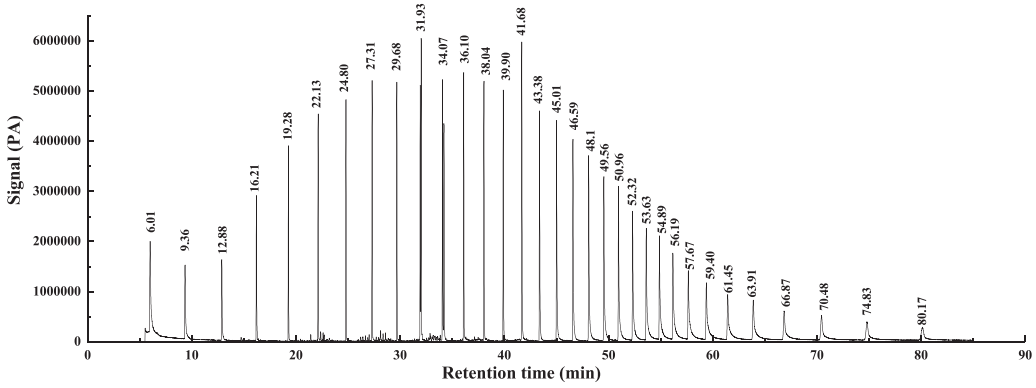

Fig. 3. Gas chromatogram of *n*-alkanes.

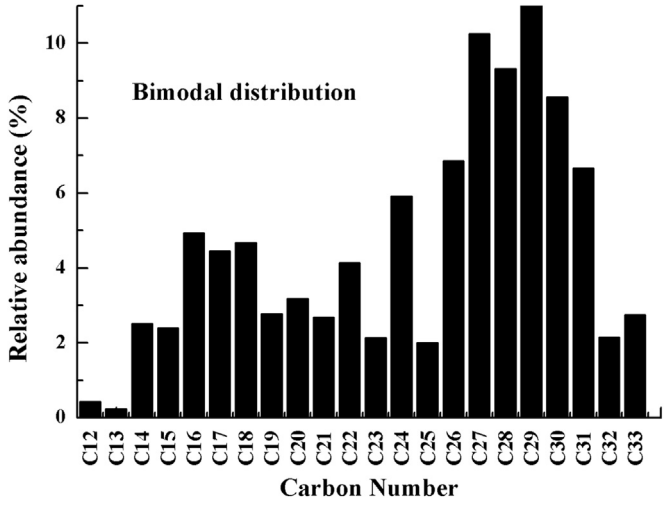

Fig. 4. Typical distribution of *n*-alkanes in the surface sediments from the YRE.

2014; Mandalakis et al., 2002; Simoneit, 1999) using the following equation: Wax $C_n = C_n - 0.5(C_{n-1} + C_{n+1})$, where negative values are treated as zero. The proportion (%) of wax derived *n*-alkanes (WNA) is expressed as the ratio between the sum of Wax C_n and the total concentrations of *n*-alkanes (Górka et al., 2014; Mandalakis et al., 2002; Simoneit, 1999).

3. Results and discussion

3.1. Concentrations and potential sources of n-alkanes in the surface sediments

n-Alkanes in the range C_{12}-C_{33} were detected in the surface sediments from the YRE. The *n*-alkanes in all the samples exhibited a bimodal distribution pattern centered at C_{16}-C_{18} and C_{26}-C_{31} (Fig. 4) without odd/even predominance. The *n*-alkanes concentrations in the surface sediments are listed in Table 1. The total *n*-alkanes concentrations ranged from 0.356 to 0.572 mg/kg, with a mean value of 0.434 mg/kg on a dry wt. basis.

Table 1
n-Alkanes concentrations (mg/kg dry wt.) and related proxies in the surface sediments from the YRE.

Sample	Concentration	MH[a]	CPI[b]	NAR[c]	WNA[d]%	P_{aq}[e]
S1	0.442	C_{27}, C_{28}, C_{29}	0.909	0	19.7	0.173
S2	0.424	C_{27}, C_{28}, C_{29}	0.924	0	17.5	0.187
S3	0.446	C_{27}, C_{28}, C_{29}	0.820	0	17.7	0.186
S4	0.446	C_{27}, C_{28}, C_{29}	0.899	0	19.9	0.177
S5	0.419	C_{27}, C_{28}, C_{29}	0.801	0	17.4	0.201
S6	0.417	C_{27}, C_{28}, C_{29}	0.835	0	19.5	0.196
S7	0.450	C_{27}, C_{28}, C_{29}	0.887	0	19.5	0.200
S8	0.426	C_{27}, C_{28}, C_{29}	0.889	0	17.9	0.203
S9	0.489	C_{27}, C_{28}, C_{29}	0.898	0	18.1	0.190
S10	0.436	C_{27}, C_{28}, C_{29}	0.839	0	19.4	0.207
S11	0.467	C_{27}, C_{28}, C_{29}	0.914	0	16.4	0.210
S12	0.520	C_{27}, C_{28}, C_{29}	1.03	0.015	19.5	0.168
S13	0.461	C_{27}, C_{28}, C_{29}	0.840	0	16.6	0.227
S14	0.572	C_{27}, C_{29}, C_{31}	1.06	0.051	23.7	0.166
S15	0.421	C_{27}, C_{28}, C_{29}	0.925	0	18.0	0.182
S16	0.388	C_{27}, C_{28}, C_{29}	0.820	0	16.9	0.182
S17	0.359	C_{27}, C_{28}, C_{29}	1.08	0.053	28.3	0.177
S18	0.356	C_{27}, C_{28}, C_{29}	1.05	0.040	27.4	0.186
S19	0.387	C_{27}, C_{28}, C_{29}	0.794	0	17.4	0.189
S20	0.388	C_{27}, C_{28}, C_{29}	0.815	0	17.0	0.181
S21	0.408	C_{27}, C_{28}, C_{29}	0.825	0	20.3	0.184

[a] Major hydrocarbons.
[b] Carbon preference index.
[c] Natural *n*-alkane ratio.
[d] Wax *n*-alkane content.
[e] Aquatic macrophytes *n*-alkane proxy.

The relatively high *n*-alkanes concentrations were recorded in sites 9, 11, 12, 13 and 14. The mean concentration of these five sites was significantly ($p = 0.000$, Table 2) higher than that of the remaining sites. These sites were all located in the area near the Hongliu Oilfield, a branch of the Shengli Oilfield. Oil spills and leakages may occur in the process of oil exploration and transportation and result in the contamination from petroleum-related hydrocarbon (Acosta-González and Marqués, 2016). Hence, these sites with high *n*-alkanes concentrations were probably influenced by the nearby Hongliu Oilfield.

In contrast, sites 15–21 had relatively low *n*-alkanes concentrations. The mean concentration of these seven sites was significantly ($p = 0.001$, Table 2) lower than that of the remaining sites. These sites were located in the area relatively far away from the Hongliu Oilfield and near the mouth of Yellow River. As mentioned above, hydrophobic organic compounds (such as *n*-alkanes) are apt to adsorb on particulate matter, especially fine particulate matter (Guo et al., 2011; Silva et al., 2013). High flow velocity and large water volume at the mouth of Yellow River are propitious for the transportation of fine suspended particles to the Bohai Sea. Hence, in addition to the low impact of the Hongliu Oilfield, the loss of a large amount of organic matter may also lead to low *n*-alkanes concentrations at these sites.

The *n*-alkanes concentrations in the surface sediments were compared with other regions in the world to assess the concentration level of aliphatic hydrocarbons in the YRE. Compared with the background concentrations, the *n*-alkanes concentrations in the YRE were similar to those in the pristine sediments of the islands in South Orkney, Antarctic (0.4 mg/kg), but lower than that in the deep basin of the Mediterranean Sea (1.1 mg/kg) (Cripps, 1994; Tolosa et al., 1996, 2004). Compared with the human-impacted locations, the *n*-alkanes concentrations in the YRE were similar to those in marine sediments in the Fladen Ground, North Sea (0.025–0.49 mg/kg; Ahmed et al., 2006) and the Bay of Marseille (0.034–2.2 mg/kg; Syakti et al., 2015). However, they were significantly lower than those in the Songhuajiang River (7.91–14.70 mg/kg; Guo et al., 2011), Ushuaia Bay (0.28–11.72 mg/kg; Commendatore et al., 2012), Jiaozhou Bay, Qingdao, China (0.50–8.20 mg/kg; Wang et al., 2006b), South Caspian Sea (0.50–17.00 mg/kg; Tolosa et al., 2004) and Bohai Sea (0.39–4.4 mg/kg; Hu et al., 2009). The comparison indicates that the concentration level of aliphatic hydrocarbons in the surface sediments of the YRE was relatively low.

Major hydrocarbons and diagnostic ratios were combined to identify the potential sources of aliphatic hydrocarbons in the surface sediments. Major hydrocarbons and related *n*-alkanes proxies are depicted in Table 1. The CPI and NAR values ranged from 0.794 to 1.08 and 0–0.0530, with a mean value of 0.897 and 0.008, respectively. Ca. 81% of samples had CPI values < 1 and NAR values of 0. A high CPI value (> 5) is indicative of a terrestrial vascular plants origin (e.g. Schefuß et al., 2003), while a low CPI value (less than or equal to 1) is considered as an input from petroleum hydrocarbons, recycled organic matter, and/or microorganisms (e.g. Fang et al., 2014). Similarly, a high NAR value (close to 1) is considered as a biogenic-related input, while petroleum hydrocarbons usually exhibited a low NAR value (close to 0; Akhbarizadeh et al., 2016; Mille et al., 2007). Based on the above analysis, both CPI and NAR values indicated a predominantly petrogenic input of hydrocarbons in the surface sediments.

In all the surface sediment samples, an evident dominance of long chain *n*-alkanes was observed. Three major hydrocarbons were identified as C_{27}, C_{28} and C_{29}. Odd *n*-alkanes were also abundant in samples (Fig. 4), considered to be indicative of biogenic source. Therefore, P_{aq} and WNA were calculated to investigate the relative contribution of different plant species to biogenic hydrocarbons.

P_{aq}, ranging from 0.166 to 0.227, reflected a mixed source including submerged/floating macrophytes, terrestrial and emergent plants based on previous studies (Ficken et al., 2000; Havelcová et al., 2015). WNA

Table 2
The results of independent samples *t*-test.

		Levene's Test for Equality of Variances		T-test for Equality of Means				
		F	Sig	t	df	Sig	Mean Difference	Std Error
Comparison A of *n*-alkanes concentrations[a]	Equal variances assumed	1.398	0.252	5.124	19	0.000	0.08864	0.01730
	Equal variances not assumed			4.102	5.139	0.009	0.08864	0.02161
Comparison B of *n*-alkanes concentrations[b]	Equal variances assumed	1.517	0.233	−4.045	19	0.001	−0.07150	0.01768
	Equal variances not assumed			−4.894	18.717	0.000	−0.07150	0.01461

[a] Comparison A : Comparison between five sites (site 9 and 11–14) and the remaining sites (site 1–8, 10 and 15–21).
[b] Comparison B : Comparison between seven sites (site 15–21) and the remaining sites (site 1–14).

was calculated to assess the proportion of terrestrial plants derived *n*-alkanes, providing strong evidence for a limited input of terrestrial higher plants (ranging from 16.4% to 28.3%).

In summary, aliphatic hydrocarbons in the surface sediments from the YRE were derived mainly from a petrogenic source, with relatively low contribution of submerged/floating macrophytes, terrestrial and emergent plants.

3.2. Concentrations and potential sources of n-alkanes in the sediment core

The dating of the sediment core was conducted using the ^{210}Pb method. The results showed that the entire core (41 cm) covered the period from 1925 to 2012. The average sedimentation rate was ca. 0.5 cm/yr. *n*-Alkanes ranging from C_8 to C_{40} were analyzed, but only C_{13}-C_{34} *n*-alkanes were detected in the sediment core. The variations in total *n*-alkanes (T-ALK), low molecular weight ($< C_{25}$, LMW) *n*-alkanes and high molecular weight ($\geq C_{25}$, HMW) *n*-alkanes concentrations are plotted vs. depth and depositional age in Fig. 5. T-ALK concentrations varied within a small range, from 0.0394 to 0.941 mg/kg (avg. 0.180 mg/kg) on a dry wt. basis. LMW and HMW *n*-alkanes concentrations ranged from 0.00556 to 0.182 and 0.0158–0.848 mg/kg dry wt. (mean 0.0687 and 0.130 mg/kg, respectively).

T-ALK concentrations were compared with those of other regions in the world. The *n*-alkanes concentrations in the OYRE were lower than the background concentrations in the world, such as the South Orkney islands in the Antarctic (0.4 mg/kg) and the Mediterranean Sea deep basin (1.1 mg/kg) (Cripps, 1994; Tolosa et al., 1996, 2004). As for the human-impacted locations, the *n*-alkanes concentrations were significant lower than those in the sediment cores from the Yellow Sea (0.70–15.80 mg/kg; Wu et al., 2001), Bohai Sea (0.88–3.48 mg/kg; Li et al., 2015), the Upper Scheldt River (2.80–29.00 mg/kg; Charriau et al., 2009), Lansquenet pond, France (2.30–29.50 mg/kg; Bertrand et al., 2012) and Chini Lake, Peninsular Malaysia (7–78 mg/kg; Bakhtiari et al., 2011). Although the sampling time and the length of sediment cores are diverse in the above mentioned areas, it can be inferred from the comparison that the concentration level of aliphatic hydrocarbons, at least roughly, was relatively low in the sediment core from the OYRE.

The depth profile of CPI is shown in Fig. 6. CPI values ranged from 0.503 to 2.11 (avg. 1.05). The low CPI values (around 1) were apparent in most samples of the core, indicating a predominant petrogenic origin. The samples in the upper section of the core (0–6 cm) showed relatively high CPI values, possibly contributing to a reduction in petroleum hydrocarbon input.

3.3. Correlation with anthropogenic activity

As illustrated in Fig. 5, the temporal trend in T-ALK concentrations is similar to that of the HMW *n*-alkanes concentrations, but different from that of the LMW *n*-alkanes concentrations. In brief, the concentrations of total, HMW and LMW *n*-alkanes sharply increased from 40 cm depth and reached a peak at 37 cm depth, where the estimated age was 1939, followed by a significant decrease until 1950 (35 cm depth). Afterwards, the HMW *n*-alkanes concentrations fluctuated slightly from 35 to 12 cm depth (over the period from 1950 to 1999). However, the total and LMW *n*-alkanes concentrations gradually increased during this period. Then, an abrupt increase in total and HMW *n*-alkanes concentrations was observed from a depth of 12 cm, followed

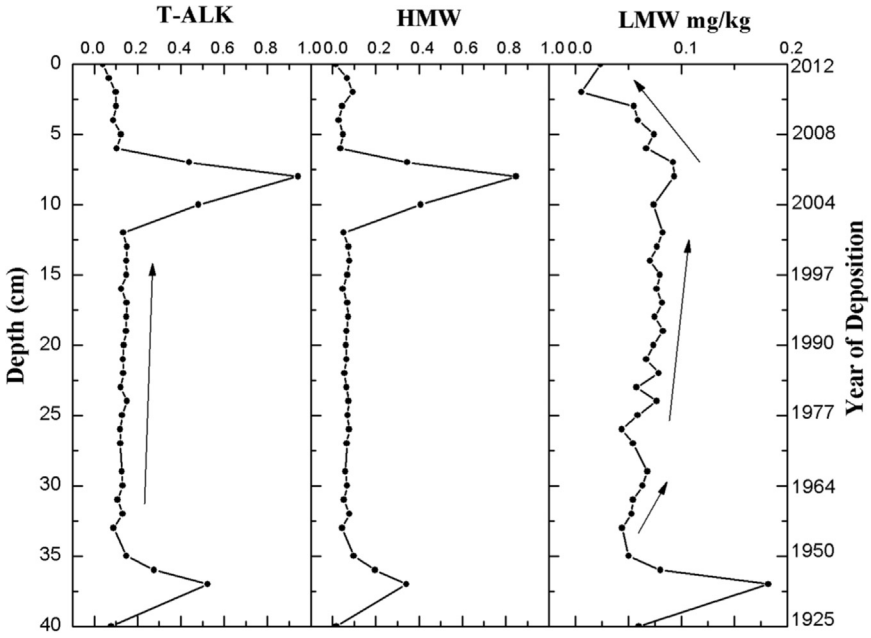

Fig. 5. Depth profile of total, HMW and LMW *n*-alkanes concentrations in the sediment core from the OYRE.

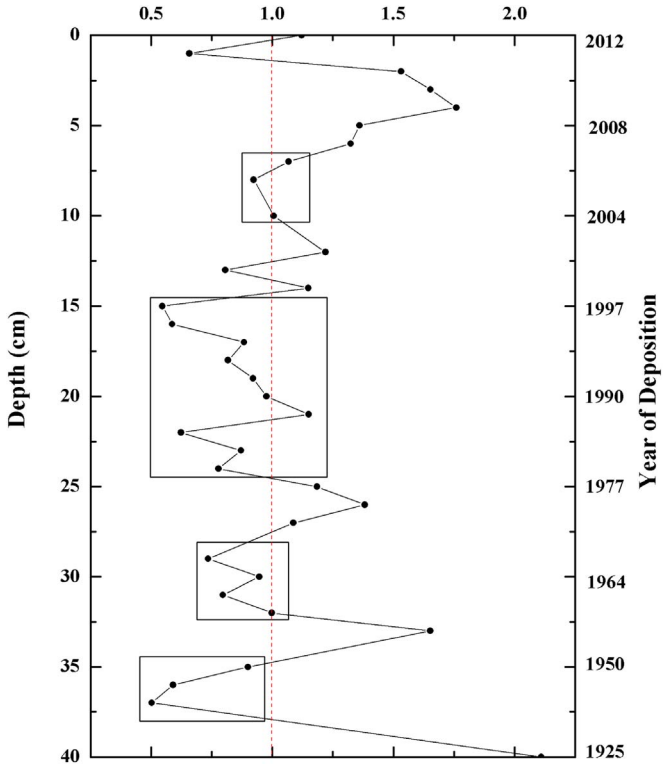

Fig. 6. Depth profile of carbon preference index (CPI) in the sediment core from the OYRE (The dot line is at CPI = 1.0; CPI value ≤1.0 indicates a petrogenic source.).

by a significant decrease to the top horizons of the core. The LMW *n*-alkanes concentrations gradually decreased with decreasing depth in the upper 6 cm layer.

The historical input of *n*-alkanes and the environmental change spanning over eight decades were recorded in the sediment core. Moreover, the depth profile of *n*-alkanes was consistent with the local and regional anthropogenic activity in the study area and the energy structure of China in the past decades. During the Second Sino-Japanese War (1937–1945), Japan occupied most regions of China, including the Shandong, Hebei and Shanxi provinces. Mineral resources, especially coal mines, were quite abundant in these regions. A number of factories, such as steel mills, sprang up there. Many prospecting and extraction activities were conducted in these regions throughout the war. Fig. 7 shows that even long chain *n*-alkanes (C_{28}, C_{30} and C_{32}) were dominant at depths of 37, 36 and 35 cm (1939, 1945 and 1950, respectively). According to previous studies, the abundance of even long chain *n*-alkanes was probably due to fossil fuel combustion (Fang et al., 2014; Wang et al., 2012a). Moreover, as shown in Fig. 6, CPI values were all < 1 at these depths, indicating a predominant petrogenic source. As a result, fossil fuel contamination resulting from the production and operation of steel mills and the exploitation of coal during this period was probably recorded in the core, which was displayed as the significant increase in *n*-alkanes concentrations around the 1940s.

An increasing trend of the total and LMW *n*-alkanes concentrations was observed over nearly half a century (35–12 cm depth, 1950–1999). In the 1960s, the Shengli Oilfield was discovered in the Yellow River Delta and exploited. The LMW *n*-alkanes concentrations significantly increased from 32 to 29 cm depth (approximately 1961–1967). Furthermore, CPI values were all < 1 during this period (Fig. 6), indicating a predominant petrogenic source. Hence, the increase in *n*-alkanes concentrations could be ascribed to the petroleum hydrocarbon input after 1961.

In 1976, an artificial diversion of Yellow River was conducted to relocate its course from Diaokou to the Qingshuigou course (Fig. 1). Yellow River then flowed into the Bohai Sea through the OYRE (Fig. 1) during the period 1976–1996. The increase in total and LMW *n*-alkanes concentrations was observed during the same period (1977–1997, 25 to 15 cm depth). Similarly, low CPI values were also apparent at depths of 25–15 cm (Fig. 6), indicating the predominant petrogenic input. With the relocation of Yellow River's course, more organic matter, including petroleum hydrocarbons, were probably transported here from the upper reaches, which may result in the increasing trend of total and LMW *n*-alkanes concentrations from 1977 to 1997. However, the slight fluctuation of HMW *n*-alkanes concentrations was observed from 25 to 15 cm depth. The significant dominance of C_{28}, C_{29}, C_{30}, C_{31} and C_{32} *n*-alkanes was observed in these layers. In general, terrestrial higher plants generally maximize at odd long chain *n*-alkanes, including C_{29} and C_{31} (Brincat et al., 2000; Wang et al., 2012b). Therefore, it can be inferred that the terrestrial higher plant input wasn't affected by the relocation of the Yellow River's course. As mentioned above, even long chain *n*-alkanes were probably derived from fossil fuel combustion (Fang et al., 2014; Wang et al., 2012a). However, fossil fuel combustion entered the estuarine sediment primarily through atmospheric deposition, which was little affected by river diversion.

The total and HMW *n*-alkanes concentrations were sharply increased from the depth of 12 cm (1999). The highest *n*-alkanes concentrations occurred at 8 cm depth (2005). Distributions of *n*-alkanes in the layers with high concentrations (10, 8 and 7 cm) are also illustrated in Fig. 7. They all showed a unimodal distribution pattern with a significant dominance of even long chain *n*-alkanes (C_{28} and C_{30}). Even long chain *n*-alkanes were generally considered to be the indicative of fossil fuel combustion (Fang et al., 2014; Wang et al., 2012a). Moreover, these layers with high *n*-alkanes concentrations also had low CPI values (around 1), suggesting the dominant petrogenic input. The Yellow River mouth was diverted again in 1996. The terminal channel of the Yellow River was shifted from the Qingshuigou course to the current course (Yellow River Estuary, Fig. 1), resulting in the decreased influence of Yellow River derived sediments on the abandoned OYRE. The studied sediment core probably well reconstructed the historical inputs of fossil fuel combustion owing to its special geographical location. To adapt to the development trend of economic globalization, China joined the World Trade Organization (WTO) in 2001, which promoted the rapid development of economy. The rapid industrial development and weak awareness of environmental protection may have exacerbated fossil fuel contamination in China during this period, which may result in the abrupt increase of *n*-alkanes concentrations from 1999 to 2007.

Over a long historical period, the energy consumption structure of China has been dominated by coal with low energy efficiency, which urges us to change energy production and consumption patterns. Moreover, developing renewable energy is important and inevitable. With the implementation of relevant environmental protection policies by the government and the enhancement of national environmental awareness, environmental contamination has generally been controlled, which may have led to the decreasing trend in *n*-alkanes concentrations after 2007 (at a depth of 6 cm).

4. Conclusion

The study showed that the concentration level of aliphatic hydrocarbons in the surface sediments of the YRE and the sediment core of the OYRE were relatively low. Surface sediment samples suffered from the contamination of petroleum hydrocarbons. The evaluation of diagnostic ratios indicated that aliphatic hydrocarbons in the surface sediments were derived mainly from a petrogenic source, with a relatively low contribution of submerged/floating macrophytes, terrestrial and emergent plants. In addition, the historical deposition of *n*-alkanes spanning over eight decades was registered in the sediment core from the abandoned OYRE. The sedimentary record of *n*-alkanes concentrations provided significant complementary information regarding the role of anthropogenic activity in environmental change. Contamination

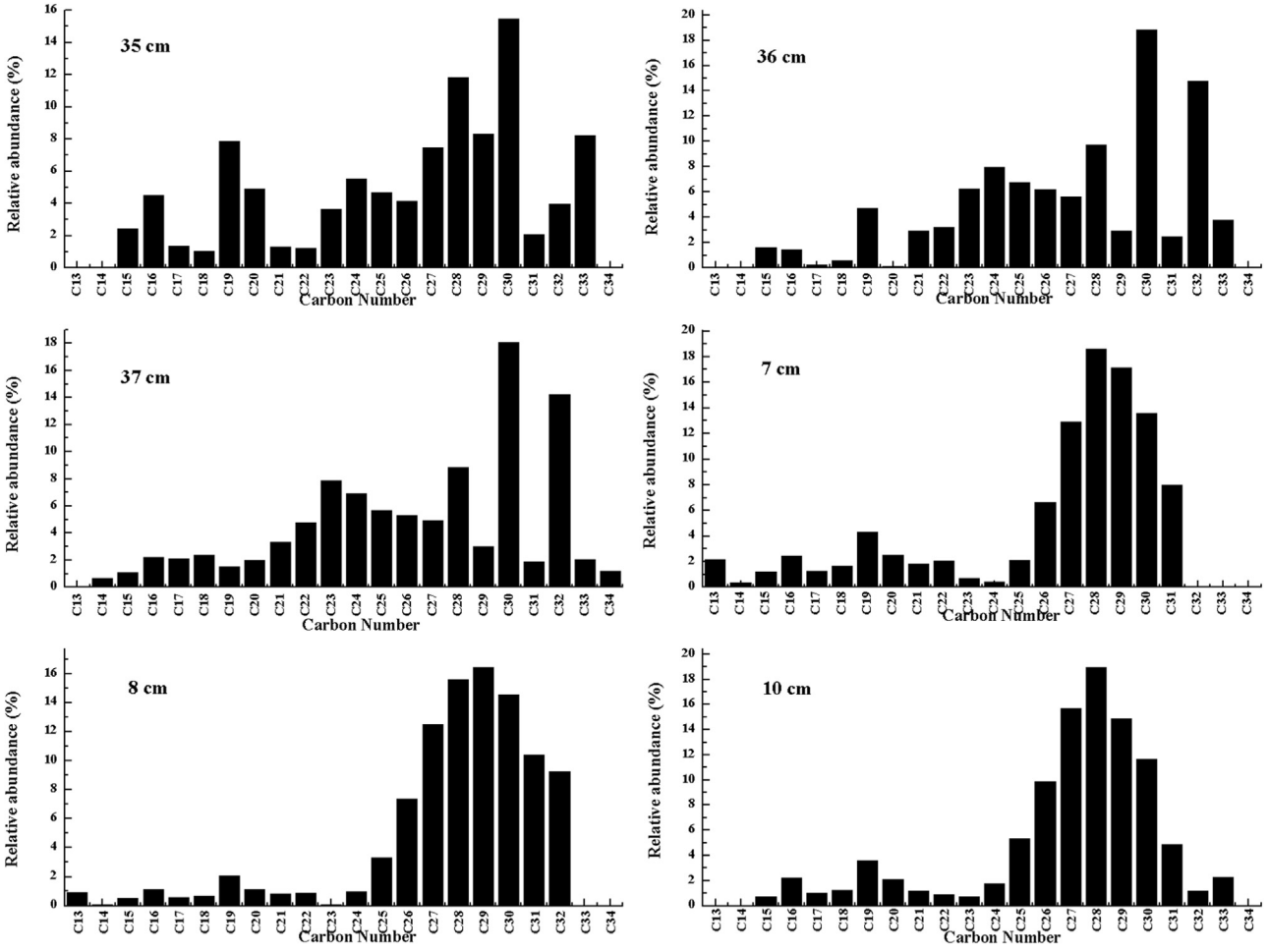

Fig. 7. Distributions of *n*-alkanes in the sediment core from the OYRE.

from fossil fuels and the side effect of China's rapid economic development were marked by the abrupt increase in *n*-alkanes concentrations. The exploitation of the Shengli Oilfield and the relocation of the Yellow River's course caused accumulation of petroleum hydrocarbons in the sediment core during 1961–1967 and 1977–1997. Overall, the systematic study of the potential sources and temporal evolution of *n*-alkanes in the surface sediments and sediment core can provide valuable insights into future investigations of other organic compounds in the Yellow River Delta. This investigation gave an assessment of the current impact of fossil fuel combustion and petroleum hydrocarbon. The obtained results may be useful for related environmental monitoring in future.

Acknowledgements

This work was supported by the National Natural Science Foundation of China (41672144). We acknowledge editors and reviewers for polishing the language of the paper and for in-depth discussion.

References

Acosta-González, A., Marqués, S., 2016. Bacterial diversity in oil-polluted marine coastal sediments. Curr. Opin. Biotechnol. 38, 24–32.

Ahmed, A.S., Webster, L., Pollard, P., Davies, I.M., Russell, M., Walsham, P., Packer, G., Moffat, C.F., 2006. The distribution and composition of hydrocarbons in sediments from the Fladen Ground, North Sea, an area of oil production. J. Environ. Monit. 8, 307–316.

Akhbarizadeh, R., Moore, F., Keshavarzi, B., Moeinpour, A., 2016. Aliphatic and polycyclic aromatic hydrocarbons risk assessment in coastal water and sediments of Khark Island, SW Iran. Mar. Pollut. Bull. 108, 33–45.

Al-Mur, B.A., Quicksall, A.N., Kaste, J.M., 2017. Determination of sedimentation, diffusion, and mixing rates in coastal sediments of the eastern Red Sea via natural and anthropogenic fallout radionuclides. Mar. Pollut. Bull.

Bakhtiari, A.R., Zakaria, M.P., Yaziz, M.I., Lajis, M.N.H., Bi, X., 2011. Variations and origins of aliphatic hydrocarbons in sediment cores from Chini Lake in Peninsular Malaysia. Environ. Forensics 12, 79–91.

Baskaran, M., Bianchi, T., Filley, T., 2017. Inconsistencies between 14C and short-lived radionuclides-based sediment accumulation rates: effects of long-term remineralization. J. Environ. Radioact. 174, 10–16.

Bertrand, O., Mansuy-Huault, L., Montargès-Pelletier, E., Losson, B., Argant, J., Ruffaldi, P., Etienne, D., Garnier, E., Dezileau, L., Faure, P., 2012. Molecular evidence for recent land use change from a swampy environment to a pond (Lorraine, France). Org. Geochem. 50, 1–10.

Brincat, D., Yamada, K., Ishiwatari, R., Uemura, H., Naraoka, H., 2000. Molecular-isotopic stratigraphy of long-chain *n*-alkanes in Lake Baikal Holocene and glacial age sediments. Org. Geochem. 31, 287–294.

Charriau, A., Bodineau, L., Ouddane, B., Fischer, J.C., 2009. Polycyclic aromatic hydrocarbons and *n*-alkanes in sediments of the Upper Scheldt River Basin: contamination levels and source apportionment. J. Environ. Monit. 11, 1086–1093.

Commendatore, M.G., Nievas, M.L., Amin, O., Esteves, J.L., 2012. Sources and distribution of aliphatic and polyaromatic hydrocarbons in coastal sediments from the Ushuaia Bay (Tierra del Fuego, Patagonia, Argentina). Mar. Environ. Res. 74, 20–31.

Cripps, G., 1994. Hydrocarbons in the Antarctic marine environment: monitoring and background. Int. J. Environ. Anal. Chem. 55, 3–13.

El Nemr, A., El-Sadaawy, M.M., Khaled, A., Draz, S.O., 2013. Aliphatic and polycyclic aromatic hydrocarbons in the surface sediments of the Mediterranean: assessment and source recognition of petroleum hydrocarbons. Environ. Monit. Assess. 185, 4571–4589.

Enrico, M., Le Roux, Gl, Heimbürger, L.-E., Van Beek, P., Souhaut, M., Chmeleff, Jr, Sonke, J.E., 2017. Holocene atmospheric mercury levels reconstructed from peat bog mercury stable isotopes. Environ. Sci. Technol. 51, 5899–5906.

Fang, J., Wu, F., Xiong, Y., Li, F., Du, X., An, D., Wang, L., 2014. Source characterization of sedimentary organic matter using molecular and stable carbon isotopic composition of *n*-alkanes and fatty acids in sediment core from Lake Dianchi, China. Sci. Total Environ. 473, 410–421.

Ficken, K.J., Li, B., Swain, D., Eglinton, G., 2000. An *n*-alkane proxy for the sedimentary

input of submerged/floating freshwater aquatic macrophytes. Org. Geochem. 31, 745–749.
Górka, M., Rybicki, M., Simoneit, B.R., Marynowski, L., 2014. Determination of multiple organic matter sources in aerosol PM_{10} from Wrocław, Poland using molecular and stable carbon isotope compositions. Atmos. Environ. 89, 739–748.
Guo, W., He, M., Yang, Z., Lin, C., Quan, X., 2011. Characteristics of petroleum hydrocarbons in surficial sediments from the Songhuajiang River (China): spatial and temporal trends. Environ. Monit. Assess. 179, 81–92.
Guo, Z., Lin, T., Zhang, G., Zheng, M., Zhang, Z., Hao, Y., Fang, M., 2007. The sedimentary fluxes of polycyclic aromatic hydrocarbons in the Yangtze River Estuary coastal sea for the past century. Sci. Total Environ. 386, 33–41.
Havelcová, M., Sýkorová, I., Mach, K., Trejtnarová, H., Blažek, J., 2015. Petrology and organic geochemistry of the lower Miocene lacustrine sediments (Most Basin, Eger Graben, Czech Republic). Int. J. Coal Geol. 139, 26–39.
Ho, S., Wang, C., Wang, M., Li, Z., 2015. Effect of petroleum on carbon and hydrogen isotopic composition of long-chain *n*-alkanes in plants from the Yellow River Delta, China. Environ. Earth Sci. 74, 1603–1610.
Hostettler, F.D., Pereira, W.E., Kvenvolden, K.A., van Geen, A., Luoma, S.N., Fuller, C.C., Anima, R., 1999. A record of hydrocarbon input to San Francisco Bay as traced by biomarker profiles in surface sediment and sediment cores. Mar. Chem. 64, 115–127.
Hu, L., Guo, Z., Feng, J., Yang, Z., Fang, M., 2009. Distributions and sources of bulk organic matter and aliphatic hydrocarbons in surface sediments of the Bohai Sea, China. Mar. Chem. 113, 197–211.
Hu, L., Guo, Z., Shi, X., Qin, Y., Lei, K., Zhang, G., 2011. Temporal trends of aliphatic and polyaromatic hydrocarbons in the Bohai Sea, China: evidence from the sedimentary record. Org. Geochem. 42, 1181–1193.
Kaiser, J., Ruggieri, N., Hefter, J., Siegel, H., Mollenhauer, G., Arz, H.W., Lamy, F., 2014. Lipid biomarkers in surface sediments from the Gulf of Genoa, Ligurian sea (NW Mediterranean sea) and their potential for the reconstruction of palaeo-environments. Deep Sea Res. Part I: Oceanogr. Res. Pap. 89, 68–83.
Li, S., Zhang, S., Dong, H., Zhao, Q., Cao, C., 2015. Presence of aliphatic and polycyclic aromatic hydrocarbons in near-surface sediments of an oil spill area in Bohai Sea. Mar. Pollut. Bull. 100, 169–175.
Mandalakis, M., Tsapakis, M., Tsoga, A., Stephanou, E.G., 2002. Gas–particle concentrations and distribution of aliphatic hydrocarbons, PAHs, PCBs and PCDD/Fs in the atmosphere of Athens (Greece). Atmos. Environ. 36, 4023–4035.
Mille, G., Asia, L., Guiliano, M., Malleret, L., Doumenq, P., 2007. Hydrocarbons in coastal sediments from the Mediterranean sea (Gulf of Fos area, France). Mar. Pollut. Bull. 54, 566–575.
Nie, M., Xian, N., Fu, X., Chen, X., Li, B., 2010. The interactive effects of petroleum-hydrocarbon spillage and plant rhizosphere on concentrations and distribution of heavy metals in sediments in the Yellow River Delta, China. J. Hazard. Mater. 174, 156–161.
Nie, M., Zhang, X.D., Wang, J.Q., Jiang, L.F., Yang, J., Quan, Z.X., Cui, X.H., Fang, C.M., Li, B., 2009. Rhizosphere effects on soil bacterial abundance and diversity in the Yellow River Deltaic ecosystem as influenced by petroleum contamination and soil salinization. Soil Biol. Biochem. 41, 2535–2542.
Renfro, A.A., Cochran, J.K., Hirschberg, D.J., Bokuniewicz, H.J., Goodbred, S.L., 2016. The sediment budget of an urban coastal lagoon (Jamaica Bay, NY) determined using 234 Th and 210 Pb. Estuar., Coast. Shelf Sci. 180, 136–149.
Salem, D.M.A., Morsy, F.A.E.M., El Nemr, A., El-Sikaily, A., Khaled, A., 2014. The monitoring and risk assessment of aliphatic and aromatic hydrocarbons in sediments of the red Sea, Egypt. Egypt. J. Aquat. Res. 40, 333–348.
Schefuß, E., Ratmeyer, V., Stuut, J.B.W., Jansen, J.F., Damsté, J.S.S., 2003. Carbon isotope analyses of *n*-alkanes in dust from the lower atmosphere over the central eastern Atlantic. Geochim. Cosmochim. Acta 67, 1757–1767.
Seki, O., Nakatsuka, T., Shibata, H., Kawamura, K., 2010. A compound-specific *n*-alkane δ13C and δD approach for assessing source and delivery processes of terrestrial organic matter within a forested watershed in northern Japan. Geochim. Cosmochim. Acta 74, 599–613.
Silva, T.R., Lopes, S.R., Spörl, G., Knoppers, B.A., Azevedo, D.A., 2013. Evaluation of anthropogenic inputs of hydrocarbons in sediment cores from a tropical Brazilian estuarine system. Microchem. J. 109, 178–188.
Simoneit, B.R., 1999. A review of biomarker compounds as source indicators and tracers for air pollution. Environ. Sci. Pollut. Res. 6, 159–169.
Syakti, A., Asia, L., Kanzari, F., Umasangadji, H., Lebarillier, S., Oursel, B., Garnier, C., Malleret, L., Ternois, Y., Mille, G., 2015. Indicators of terrestrial biogenic hydrocarbon contamination and linear alkyl benzenes as land-base pollution tracers in marine sediments. Int. J. Environ. Sci. Technol. 12, 581–594.
Tahir, N.M., Pang, S., Simoneit, B., 2015. Distribution and sources of lipid compound series in sediment cores of the southern South China Sea. Environ. Sci. Pollut. Res. 22, 7557–7568.
Tolosa, I., Bayona, J.M., Albaigés, J., 1996. Aliphatic and polycyclic aromatic hydrocarbons and sulfur/oxygen derivatives in northwestern Mediterranean sediments: spatial and temporal variability, fluxes, and budgets. Environ. Sci. Technol. 30, 2495–2503.
Tolosa, I., de Mora, S., Sheikholeslami, M.R., Villeneuve, J.P., Bartocci, J., Cattini, C., 2004. Aliphatic and aromatic hydrocarbons in coastal Caspian Sea sediments. Mar. Pollut. Bull. 48, 44–60.
Wang, C., Wang, W., He, S., Du, J., Sun, Z., 2011. Sources and distribution of aliphatic and polycyclic aromatic hydrocarbons in Yellow River Delta Nature Reserve, China. Appl. Geochem. 26, 1330–1336.
Wang, H., Yang, Z., Li, G., Jiang, W., 2006a. Wave climate modeling on the abandoned Huanghe (Yellow River) delta lobe and related deltaic erosion. J. Coast. Res. 22, 906–918.
Wang, J.Z., Yang, Z.Y., Chen, T.H., 2012a. Source apportionment of sediment-associated aliphatic hydrocarbon in a eutrophicated shallow lake, China. Environ. Sci. Pollut. Res. 19, 4006–4015.
Wang, M., Wang, C., Hu, X., Zhang, H., He, S., Lv, S., 2015. Distributions and sources of petroleum, aliphatic hydrocarbons and polycyclic aromatic hydrocarbons (PAHs) in surface sediments from Bohai Bay and its adjacent river, China. Mar. Pollut. Bull. 90, 88–94.
Wang, S.S., Liu, G.J., Y, Z.J., Da, C.N., 2017. Distribution, origin, and characteristics of *n*-alkanes in surface soils from the Yellow River Delta natural reserve, China. Soil Sci. Soc. Am. J. 81, 915–922.
Wang, X.C., Sun, S., Ma, H.Q., Liu, Y., 2006b. Sources and distribution of aliphatic and polyaromatic hydrocarbons in sediments of Jiaozhou Bay, Qingdao, China. Mar. Pollut. Bull. 52, 129–138.
Wang, Y., Zhu, L., Wang, J., Ju, J., Lin, X., 2012b. The spatial distribution and sedimentary processes of organic matter in surface sediments of Nam Co, Central Tibetan Plateau. Chin. Sci. Bull. 57, 4753–4764.
Wu, X., Bi, N., Kanai, Y., Saito, Y., Zhang, Y., Yang, Z., Fan, D., Wang, H., 2015. Sedimentary records off the modern Huanghe (Yellow River) delta and their response to deltaic river channel shifts over the last 200 years. J. Asian Earth Sci. 108, 68–80.
Wu, Y., Zhang, J., Mi, T.Z., Li, B., 2001. Occurrence of *n*-alkanes and polycyclic aromatic hydrocarbons in the core sediments of the Yellow Sea. Mar. Chem. 76, 1–15.
Yamei, H., ZHENG, M., Zhengtao, L., Lirong, G., 2009. Distribution of polycyclic aromatic hydrocarbons in sediments from Yellow River Estuary and Yangtze River Estuary, China. J. Environ. Sci. 21, 1625–1631.
Yu, S., Li, S., Tang, Y., Wu, X., 2011. Succession of bacterial community along with the removal of heavy crude oil pollutants by multiple biostimulation treatments in the Yellow River Delta, China. J. Environ. Sci. 23, 1533–1543.
Zhang, L., Zhang, J., Gong, M., 2009. Size distributions of hydrocarbons in suspended particles from the Yellow River. Appl. Geochem. 24, 1168–1174.